Translational Oncology 33 (2023) 101676

Contents lists available at ScienceDirect

Translational Oncology

journal homepage: www.elsevier.com/locate/tranon

Original Research

G0S2 promotes antiestrogenic and pro-migratory responses in ER+ and ER- breast cancer cells

Andrea K. Corbet [a], Emmanuel Bikorimana [a], Raya I. Boyd [a], Doha Shokry [a], Kelly Kries [a], Ayush Gupta [a], Anneliese Paton [a], Zhengyang Sun [a], Zeeshan Fazal [a], Sarah J. Freemantle [a], Erik R. Nelson [b,c,d,e], Michael J. Spinella [a,c,d,e,*], Ratnakar Singh [a,*]

[a] Department of Comparative Biosciences, University of Illinois Urbana-Champaign, Urbana, IL, 61801, USA
[b] Department of Molecular and Integrative Physiology, University of Illinois Urbana-Champaign, Urbana, IL 61801, USA
[c] Carle Illinois College of Medicine University of Illinois Urbana-Champaign, Urbana IL 61801, USA
[d] Carl R. Woese Institute for Genomic Biology, Anticancer Discovery from Pets to People Theme, University of Illinois Urbana-Champaign, Urbana IL 61801, USA
[e] Cancer Center of Illinois, University of Illinois Urbana-Champaign, Urbana IL 61801, USA

ARTICLE INFO

Keywords:
G0S2
Breast cancer
Estrogen receptor
Antiestrogen
Epithelial mesenchymal transition

ABSTRACT

G0/G1 switch gene 2 (G0S2) is known to inhibit lipolysis by inhibiting adipose triglyceride lipase (ATGL). In this report, we dissect the role of G0S2 in ER+ versus ER- breast cancer. Overexpression of G0S2 in ER- cells increased cell proliferation, while G0S2 overexpression in ER+ cells decreased cell proliferation. Transcriptome analysis revealed that G0S2 mediated distinct but overlapping transcriptional responses in ER- and ER+ cells. G0S2 reduced genes associated with an epithelial phenotype, especially in ER- cells, including CDH1, ELF3, STEAP4 and TACSTD2, suggesting promotion of the epithelial-mesenchymal transition (EMT). G0S2 also repressed estrogen signaling and estrogen receptor target gene signatures, especially in ER+ cells, including TFF1 and TFF3. In addition, G0S2 overexpression increased cell migration in ER- cells and increased estrogen deprivation sensitivity in ER+ cells. Interestingly, two genes downstream of ATGL in fat utilization and very important in steroid hormone biosynthesis, HMGCS1 and HMGCS2, were downregulated in G0S2 overexpressing ER+ cells. In addition, HSD17B11, a gene that converts estradiol to its less estrogenic derivative, estrone, was highly upregulated in G0S2 overexpressing ER+ cells, suggesting G0S2 overexpression has a negative effect on estradiol production and maintenance. High expression of G0S2 and HSD17B11 was associated with improved relapse-free survival in breast cancer patients while high expression of HMGSC1 was associated with poor survival. Finally, we deleted G0S2 in breast cancer-prone MMTV-PyMT mice. Our data indicates a complex role for G0S2 in breast cancer, dependent on ER status, that may be partially mediated by suppression of the estrogen signaling pathway.

Introduction

Breast cancer has the second-highest cancer mortality rate in women in the United States, superseded only by lung cancer [1]. Breast cancer is often categorized by cellular receptor expression, with about 70% of breast cancers being hormone receptor-positive (ER+/PR+) and human epidermal growth receptor 2-negative (HER2-), about 15% are ER-/HER2+, and 5–10% triple-negative (TNBC) [1,2]. Most standard treatments for breast cancer are receptor-targeting therapies, such as tamoxifen, a selective estrogen receptor modulator for ER+ cancers, or trastuzumab (Herceptin) for HER2+ cancers [3]. TNBC has a worse prognosis compared to ER+ breast cancer due to the lack of therapeutic targets and is associated with high-grade disease and aggressive metastasis [4]. However, despite a better prognosis, therapy resistance in ER+ breast cancer does occur, particularly resistance to endocrine therapy, and a portion of patients will experience relapse within 2 to 10 years after primary treatment [1,5]. There is an extensive effort to better understand therapy resistance and relapse to identify biomarkers that can aid in patient prognosis, as well as identify new therapeutic targets in ER+ and TNBC.

G0/G1 switch gene 2 (G0S2) was first identified in lymphocytes during the drug-induced transition from the G0 to G1 phase of the cell cycle, associating the protein with cell-cycle regulation [6]. G0S2 is

* Corresponding authors at: Department of Comparative Biosciences, University of Illinois Urbana-Champaign, 2001 South Lincoln Street, Urbana, IL 61802, USA.
E-mail addresses: spinella@illinois.edu (M.J. Spinella), rsingh02@illinois.edu (R. Singh).

https://doi.org/10.1016/j.tranon.2023.101676
Received 22 December 2022; Received in revised form 12 April 2023; Accepted 14 April 2023
Available online 20 April 2023

Abbreviations

ATGL	adipose triglyceride lipase
EMT	epithelial-mesenchymal transition
ER	estrogen receptor
G0S2	G0/G1 switch gene 2
GSEA	gene set enrichment analysis
MEF	murine embryonic fibroblast
MMTV	mouse mammary tumor virus
PyMT	polyoma middle T antigen (PyMT)
TNBC	triple-negative breast cancer

comprised of 103 amino acids and is highly conserved in vertebrates with no known homologs in invertebrates [7]. The tertiary structure of the G0S2 protein is unknown but proposed to consist of alpha-helices and unstructured regions [8,9]. Since its identification, G0S2 has been associated with several cellular processes, including cell-cycle regulation, inflammation, lipolysis, and cancer [6,7,10–13]. G0S2 has been extensively studied as a direct inhibitor of adipose triglyceride lipase (ATGL) [14,15], the rate-limiting enzyme in cellular triglyceride breakdown. G0S2 null mice have alterations in adiposity, energy balance, and thermogenesis [14,16].

G0S2 is also silenced by gene promoter methylation in a variety of solid tumors and has been associated with terminal differentiation, cell cycle withdrawal, quiescence, and apoptosis [13,17–29]. G0S2 is a direct retinoic acid target gene associated with retinoic acid-mediated clinical remissions in acute promyelocytic leukemia [30,31]. Utilizing G0S2 null murine embryonic fibroblasts (MEFs) we demonstrated that G0S2 has properties of a classical tumor suppressor by antagonizing oncogene induced transformation [32]. G0S2 null MEFs have increased susceptibility to undergo transformation with mutated HRAS (V12) or EGFR. This activity of G0S2 was independent of ATGL [32]. We reported a role for G0S2 in ER+ breast cancer suppression as low G0S2 expression correlated with increased recurrence after antiestrogen therapy, and stable G0S2 overexpression sensitized ER+ breast cancer cells to tamoxifen and PI3K/mTOR inhibitors [33]. However, some reports suggest that G0S2 may also have tumor promoting properties, including one report that G0S2 knockdown in ER- MDA-MB-231 cells inhibited cell migration and epithelial-mesenchymal transition (EMT) [34–38].

In this report, we directly compare the effects of inducible G0S2 expression in ER+ and ER- breast cancer cells. Overexpression of G0S2 in ER- breast cancer cells increased cell proliferation while G0S2 overexpression in ER+ breast cancer cells decreased cell proliferation. G0S2 mediated distinct but overlapping transcriptional responses in ER+ and ER- cells. This included promoting a more mesenchymal phenotype associated with cell migration, especially in ER- cells, and suppressing estrogen signaling, especially in ER+ cells. A major finding is that G0S2 overexpression was associated with reduced estradiol availability by altering levels of key enzymes in steroidogenesis. The antiestrogen effects apparently override the cancer promoting EMT effects in ER+ cells that are highly dependent on estrogen for growth and survival. This finding suggests that G0S2 may not only promote triglyceride storage but may also have a role in regulating local cholesterol and steroid hormones levels. In summary, our findings support a complex and cell context dependent role for G0S2 for both tumor promotion and suppression that we hypothesize may be mediated in part by local control of both fat degradation and cholesterol formation. In addition, our findings suggest an intriguing mechanism for G0S2 suppression of ER+ cells, namely limiting local estrogen availability.

Materials and methods

Derivation of G0S2 inducible cells

ER+ T47D and ER- MDA-MB-231 cells were purchased from ATCC and maintained in high-glucose DMEM (Sigma) supplemented with 10% FBS (Invitrogen), 1% antibiotics (Corning), and 1% L-glutamine (Corning). Tet-on system plasmids were purchased from VectorBuilder, and lentiviral stocks were generated using HEK293T cells as previously described [39]. The constructs were TRE-G0S2(pLV-Hygro--TRE3G>hG0S2[NM_015714.3]) and TET-3G(pLV-Bsd-CMV>Tet3G). Lentivirus was added sequentially to target cells and selected sequentially in 7.0 μg/mL blasticidin followed by 3.0 μg/mL hygromycin. Tet-on inducible cells were maintained in tetracycline-free FBS (R&D Systems) media. Pilot experiments determined that 0.5 μg/mL doxycycline was sufficient for robust induction of G0S2 expression in both T47D and MDA-MB-231 cells as determined by Western blot (Fig. 1A).

Cell proliferation assays

Cells were treated with 0.5 μg/mL doxycycline for 15 days and then assessed for cell proliferation by CellTiter-Glo (Promega). The time point of 15 days of G0S2 induction was chosen as pilot experiments determined that prominent proliferative effects did not begin until 12 days of G0S2 induction. Briefly, an equal number of cells were plated in 24-well plates in four biological replicates at 20,000 cells per well, and viable cell numbers were estimated for 6 consecutive days using the CellTiter-Glo assay. Estrogen-depleted assays were performed by replacing standard media with phenol red-free media (Sigma), charcoal-stripped FBS (Invitrogen), and 1% sodium pyruvate (Corning) one day after cell plating.

RNA-sequencing and gene set enrichment and gene signature analysis

RNA was extracted from cells in biological triplicate using the RNeasy Mini Kit (Qiagen). RNA sequencing was performed by the Roy J. Carver Biotechnology Center. RNA-seq libraries were prepared using the TruSeq Stranded mRNA Sample Prep kit (Illumina). The libraries were sequenced on a HiSeq 4000 using HiSeq 4000 sequencing kit version 1. Quality control of reads generated from RNA sequencing was performed using FASTQC. Trimmomatic was used to remove the low-quality bases from starts and ends with a threshold of LEADING <28 and TRAILING <28, respectively, with a minimum length of 30. The resulting clean reads were then aligned to human genome assembly NCBI GRCh38.p12 using STAR aligner. The resulting aligned reads from STAR aligner were used to count the reads mapping to each gene in each sample using feature counts. All the samples have comparable numbers of reads and comparable quality scores. The mean quality value across each base position in the read was >30 representing a 99.9% base call accuracy. Differentially expressed genes were identified by Limma Bioconductor package. The RNA-seq datasets from this study have been submitted to the NCBI Database of GEO Datasets (GSE227698). Gene set enrichment analysis (GSEA) was performed using a maximum and minimum gene set size of 500 and 15, respectively. The number of permutations was 1000 and the permutation type was gene_set.

Western blots and real-time PCR

For Western blots, cells were lysed in radioimmune precipitation (RIPA) buffer and separated by SDS-PAGE. RIPA buffer consisted of 50 mM Tris–HCl, 150 mM NaCl, 0.5% (w/v) sodium deoxycholate, 1.0% (v/v) NP-40, 1.0 mM EDTA, 0.1% (w/v) SDS, and 0.01% (w/v) sodium azide at a pH of 7.4. A 100X Protease and phosphatase inhibitor cocktail was added to RIPA buffer just before use. G0S2 antibody (12,091-AP) was purchased from ProteinTech and the actin antibody was from Thermo Fisher (MA1–744). For real-time PCR, total cellular RNA was

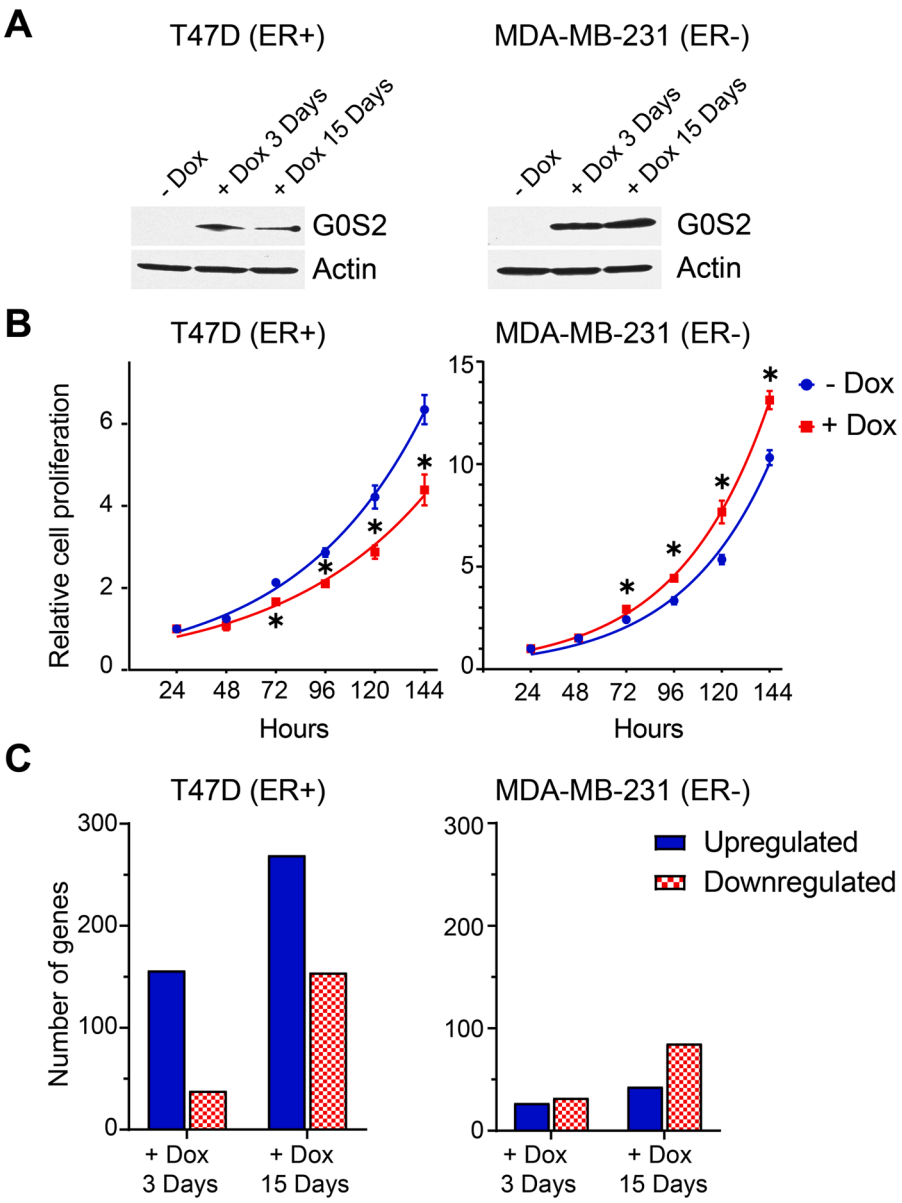

Fig. 1. Inducible expression of G0S2 has contrasting effects on proliferation of ER- and ER+ cells. (A) G0S2 Immunoblot of ER- MDA-MB-231 and ER+ T47D cells after doxycycline (Dox) induction of G0S2 for 3 and 15 days. (B) Cell proliferation and viability assays of MDA-MB-231 and T47D cells after 15-day induction of G0S2. Data represent mean +/- standard error of the mean of four biological replicates and normalized to the 24-hour time point. Two-tailed student's t-tests were performed for statistical analysis. $^*P \leq 0.05$. All experiments were repeated at least twice with similar results. (C) Total number of upregulated and downregulated genes after 3 and 15 days of G0S2 induction in MDA-MB-231 and T47D cells. RNA-seq was performed in biological triplicate. A 1.5-fold cut-off and $P < 0.05$ was used.

isolated using the RNeasy Mini Kit (Qiagen), and complementary DNAs (cDNAs) were synthesized using High-Capacity cDNA Reverse Transcription Kit iScript Reverse Transcription Supermix (Thermo Fisher ScientificBio-Rad Laboratories). Quantitative real-time PCR assays were performed with PowerUp SYBR Green Master Mix iTaq Universal SYBR Green Supermix (Thermo Fisher ScientificBio-Rad Laboratories) and the QuantStudio 3 Real-time System (Thermo Fisher) normalized to GAPDH as described [39]. Primer sequences are available on request.

In silico and survival analysis

The 1903 patient METABRIC breast cancer dataset from TCGA was assessed via cBioPortal. High expressions of G0S2, HSD17B11, and HMGSC1 were each defined as 1.0 SD above the mean and Kaplan–Meier log-rank tests were performed using the cBioPortal survival web tool. The cBioPortal co-expression web tool and the METABRIC dataset were used to assess the co-expression patterns of G0S2, HSD17B11, and HMGSC1.

Wound healing assay

T47D cells and MDA-MB-231 cells were plated in 24-well plates with silicone inserts (Ibidi) to provide uniform wounds, and the assay was carried out according to the provided protocol. Images were obtained immediately after the inserts were removed, then every 9 h for MDA-231 cells and every 24 h for T47D cells.

Estrone ELISA

Uninduced and induced cells were seeded at 300,000 cells per well in six-well plates in phenol red-free media with charcoal-stripped FBS and supplemented with 1.0 pM estradiol (Sigma). A competitive estrone ELISA kit was purchased from Invitrogen and performed according to the provided protocol. Estrone concentrations were normalized to cell number.

PyMT-MMT G0S2 mice

All animal experiments were approved by the University of Illinois Animal Care and Usage Committee (IACUC) under protocol number 20143. Male MMTV-PyMT transgenic mice of C57BL/6 background (The Jacksons Laboratory) were paired with previously described heterozygous G0S2 females of the same background [16]. Briefly, G0S2+/− mice in the C57Bl/6 strain background were generated by the trans-National Institute of Health (NIH) Knockout Mouse Project (KOMP) and obtained from the KOMP Repository. G0S2-null VGB6 embryonic stem (ES) cells isolated from the C57Bl/6NTac mouse strain were generated by KOMP. The G0S2 coding region was replaced by a lacZ and loxP-flanked neomycin resistance gene cassette and the lacZ gene was fused in-frame at the G0S2 ATG start codon. Targeting was confirmed by PCR analyses and these cells were injected into Albino C57Bl/6 blastocysts and transferred into pseudo-pregnant recipient mice. Mice with a high degree of coat color chimerism were bred with C57Bl/6 mice to test for germ line transmission. F1 mice G0S2+/− were intercrossed to generate G0S2+/+, G0S2+/−, and G0S2−/− mice. The G0S2−/− genotype was confirmed by PCR analysis of tail tip DNA using DNeasy Blood and Tissue Kit (Qiagen, 69504) and HotStar taq DNA polymerase (Qiagen, 203203). Age- and gender-matched mice were used for the described experiments. All mice were housed in a standard pathogen-free facility on a 12 h light 12 h dark cycle and they had continuous access to water and regular food chow (Harlan Laboratories). Protocols for the animal studies were approved by the University of Illinois IACUC. Genotyping was performed on tail-snipped DNA. PCR was carried out using the Kapa2G Hotstart PCR kit using the following primers (mouse G0S2: F:5′-CTGCGGGAAGCGTGTGAA-3′ R: 5′-ATC ACAGTGCGTGCTGCA-3′, mouse LAC-Z: F: 5′-GGTAAACTGGCTCGGA TTAGG-3′ R: 5′-TTGACTCTAGCGGCTGATGTT-3′, MMTV-PyMT transgene: F: 5′-GGAAGCAAGTACTTCACAAGGG-3′ R: 5′-GGAAAGTCACT AGGAGCAGGG-3′, internal control: F: 5′-CAAATGTTGCTTGTC TGGTG-3′ R: 5′-GTCAAGTCGAGTGCACAGTTT-3′).

Transgene-positive females were monitored for tumors once a week, starting at two months of age. Tumor screening was done by scruffing and palpating the abdomen and neck area along the mammary glands. Tumors were individually measured using electronic calipers by taking two measurements on perpendicular planes of the tumor, with the smaller measurement being considered the width. The formula (L x W x W)/2 was used to calculate the tumor volume. Tumors were allowed to progress for six weeks, sacrificed according to DAR protocols, and all tumors were removed. All tumors were weighed collectively for a total tumor burden, and the largest tumor was weighed separately for maximum tumor weight. Lungs were assessed for the presence or absence of visible metastases. The final statistical analysis was performed with GraphPad Prism 9.3.0 using Kruskal-Wallis multiple comparison test for tumor initiation, unpaired t-tests for tumor growth, and 2-way ANOVAs for tumor weight.

Statistics

Two-tailed student's t-tests, one-way or two-way ANOVA with post hoc Bonferroni, and log-rank tests were performed where appropriate using GraphPad Prism v6.0 and P-values indicative of non-significant $P > 0.05$ and significant $^*P \leq 0.05$ were determined. Mean and the standard error of the mean was used to describe sample variability. For a 2 × 2 factorial design with sample size of 7 per treatment group, this study achieves 80% at alpha=0.05 to detect an effect size of 0.55.

Results

Inducible G0S2 expression has contrasting effects on the proliferation of ER- and ER+ breast cancer cells

We previously reported decreased G0S2 expression in breast cancer patients compared to normal breast tissue and that G0S2 expression correlated with improved relapse free survival in ER+ breast cancer patients and had a tumor suppressive effect on ER+ breast cancer cells [32,33]. While G0S2 has been shown to be commonly silenced by DNA methylation and to have a tumor suppressive function in various cancers [17–29], other reports including a report on MDA-MB-231 ER- breast cancer cells, suggests a pro-cancer role for G0S2 [38]. To directly compare the effects of G0S2 in ER+ and ER- cells we generated ER+ T47D and ER- MDA-MB-231 cells with inducible expression of G0S2 (Fig. 1A). Cell proliferation was monitored after 15 days of G0S2 induction. MDA-MB-231 cells had higher basal proliferation compared to T47D cells. While G0S2 overexpression resulted in a decrease in the rate of proliferation of T47D cells, in agreement with our prior results [33], the opposite effect was seen in MDA-MB-231 cells which had increased cell proliferation with G0S2 induction (Fig. 1B). To assess potential mechanisms to account for the disparate effects of G0S2 overexpression in ER+ and ER- breast cancer cells we performed RNA-seq in both T47D and MDA-MB-231 cells after 3 and 15 days of G0S2 induction. In general, T47D cells appeared more responsive to G0S2 induction with 156 and 269 genes upregulated and 38 and 154 genes downregulated with a fold-change greater than 1.5 and a $P < 0.05$, after 3 and 15 days respectively. In comparison, there were only 27 and 43 genes upregulated and 32 and 85 downregulated in MDA-MB-231 cells after 3 and 15 days (Fig. 1C).

Inducible G0S2 expression downregulates genes involved with an apical and epithelial phenotype, especially in ER- cells, and promotes cell migration

We performed gene set enrichment analysis (GSEA) on T47D and MDA-MB-231 cells after G0S2 induction using the human MSigDB Hallmark database. MDA-MB-231 cells demonstrated a prominent repression of gene sets related to the apical epithelium at 3 and 15 days of G0S2 induction. These gene sets included EPITHELIAL_MESNECHYMAL_TRANSITION and APICAL_JUNCTION (Fig. 2A). RT-PCR confirmed that epithelial genes normally repressed during epithelial mesenchymal transition (EMT) had reduced expression after G0S2 induction, including ELF3, STEAP4 and TACSTD2, and the master regulator of the epithelial phenotype, E-cadherin (CDH1) (Fig. 2B). This repression in epithelial genes correlated with increased cell migration after G0S2 induction in MDA-MB-231 cells (Fig. 2C). This result is consistent with a prior report demonstrating an increase in E-cadherin and a decrease in cell migration upon siRNA knockdown of G0S2 in MDA-MB-231 cells [38]. Decreased enrichment of epithelial genes was also seen in T47D cells (Figs. 3A and S1). Interestingly, G0S2 induction resulted in a decrease in cell migration in T47D cells (Figure S1), which may be due to a significant anti-estrogen effect of G0S2 (see below). In summary, G0S2 appears to have an EMT-related, cancer promoting activity that manifests primarily in estrogen independent cells.

G0S2 expression downregulates the expression of ER target genes and genes involved in hormone synthesis and upregulates a gene involved in estradiol conversion to estrone

GSEA analysis of T47D cells after G0S2 induction demonstrated prominent repression of gene sets related to estrogen receptor target genes including ESTROGEN_RESPONSE_EARLY and ESTROGEN_RESPONSE_LATE (Fig. 3A). RT-PCR confirmed that several direct ER target genes were downregulated in T47D cells after G0S2 induction including TFF1 and TFF3 (Fig. 3B). Interestingly the cytosolic and mitochondrial forms of 3-hydroxy-3-methylglutaryl-CoA synthase (HMGCS1 and HMGCS2, respectively) were both substantially downregulated after G0S2 induction in T47D cells. HMGCS catalyzes an important step in cholesterol biosynthesis which in turn is a precursor for steroid hormones including estrogen [40]. and

A

MDA-MB-231 (ER-)

GENE SETS REPRESSED 3 DAYS AFTER G0S2 INDUCTION	SIZE	NES	p-val
HALLMARK_E2F_TARGETS	199	-1.682	0.000
HALLMARK_INFLAMMATORY_RESPONSE	129	-1.667	0.000
HALLMARK_MYC_TARGETS_V2	56	-1.663	0.002
HALLMARK_MYC_TARGETS_V1	198	-1.503	0.000
HALLMARK_G2M_CHECKPOINT	198	-1.491	0.000
HALLMARK_IL6_JAK_STAT3_SIGNALING	56	-1.289	0.112
HALLMARK_EPITHELIAL_MESENCHYMAL_TRANSITION	163	-1.206	0.100

MDA-MB-231(ER-)

GENE SETS REPRESSED 15 DAYS AFTER G0S2 INDUCTION	SIZE	NES	p-val
HALLMARK_INFLAMMATORY_RESPONSE	129	-1.905	0.000
HALLMARK_EPITHELIAL_MESENCHYMAL_TRANSITION	163	-1.823	0.000
HALLMARK_APICAL_JUNCTION	150	-1.760	0.000
HALLMARK_ESTROGEN_RESPONSE_LATE	162	-1.693	0.000
HALLMARK_ESTROGEN_RESPONSE_EARLY	171	-1.673	0.000
HALLMARK_IL6_JAK_STAT3_SIGNALING	56	-1.588	0.009
HALLMARK_MYOGENESIS	124	-1.561	0.001

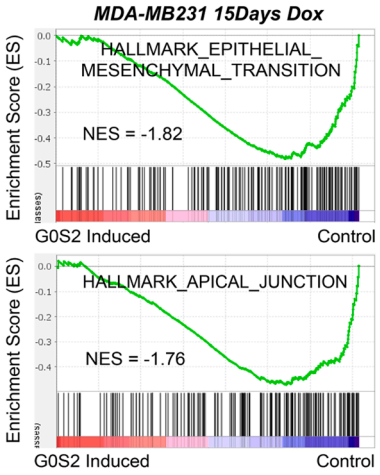

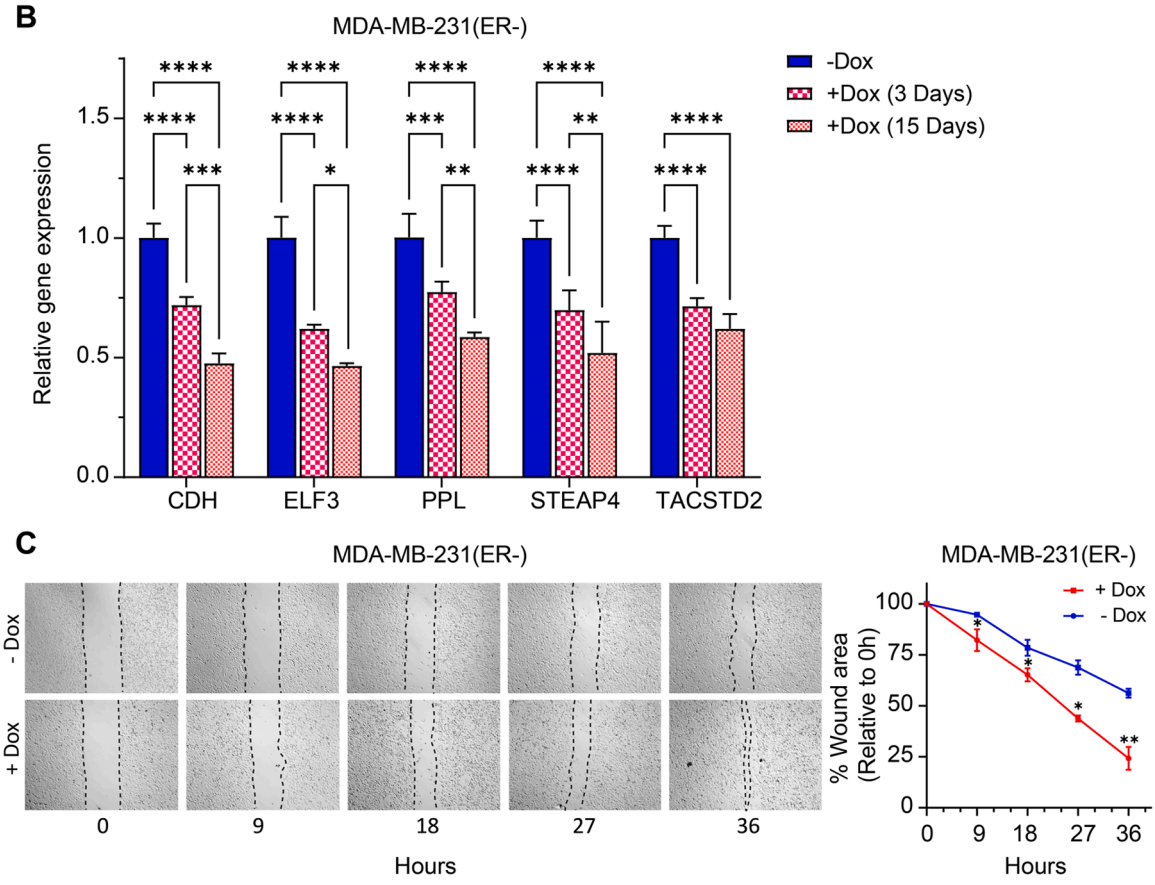

Fig. 2. Inducible G0S2 expression in ER- cells downregulates genes involved in an apical and epithelial phenotype and promotes cell migration. (A) Gene set enrichment analysis (GSEA) showing the top 7 HALLMARK gene sets ranked by normalized enrichment score (NES) downregulated in MDA-MB-231 cells at 3 and 15 days of G0S2 induction. Representative gene set enrichment plots for EPITHELIAL_MESNECHYMAL_TRANSITION and APICAL_JUNCTION. (B) Real-time PCR confirmation that epithelial genes normally repressed during epithelial mesenchymal transition (EMT) are downregulated after G0S2 induction in MDA-MB-231 cells. Data represent mean +/- standard error of the mean of three biological replicates. Two-tailed student's t-tests were performed for statistical analysis. Experiments were repeated at least twice with similar results. (C) G0S2 induction increased cell migration of MDA-MB-231 cells. Cell invasion was assessed as described in Methods. Data represent mean +/- standard error of the mean of three biological replicates. Representative of two independent experiments. $^{*}P \leq 0.05$, $^{**}P \leq 0.01$, $^{***}P \leq 0.005$, $^{****}P \leq 0.001$.

27-hydroxychoeslterol, and oxysterol that can activate the estrogen receptor in models of breast cancer [41,42]. In addition, there was an over 10-fold induction in hydroxysteroid 17-beta dehydrogenase 11 (HSD17B11) also commonly called estradiol 17-beta-dehydrogenase 11, an enzyme known to convert estradiol into the less potent estrogen, estrone (Fig. 3B) [43–45]. In accordance with this finding the level of estrone was increased approximately 50-fold in T47D cells upon G0S2 induction (Fig. 3C) and the negative effect of G0S2 on T47D cell proliferation was greatly exacerbated under estrogen deprived culture conditions (Fig. 3D), which could be rescued by addition of exogenous estrogen (Fig. 3E). In contrast, while ER target gene data sets were also repressed in MDA-MB-231 cells upon G0S2 induction, there was less

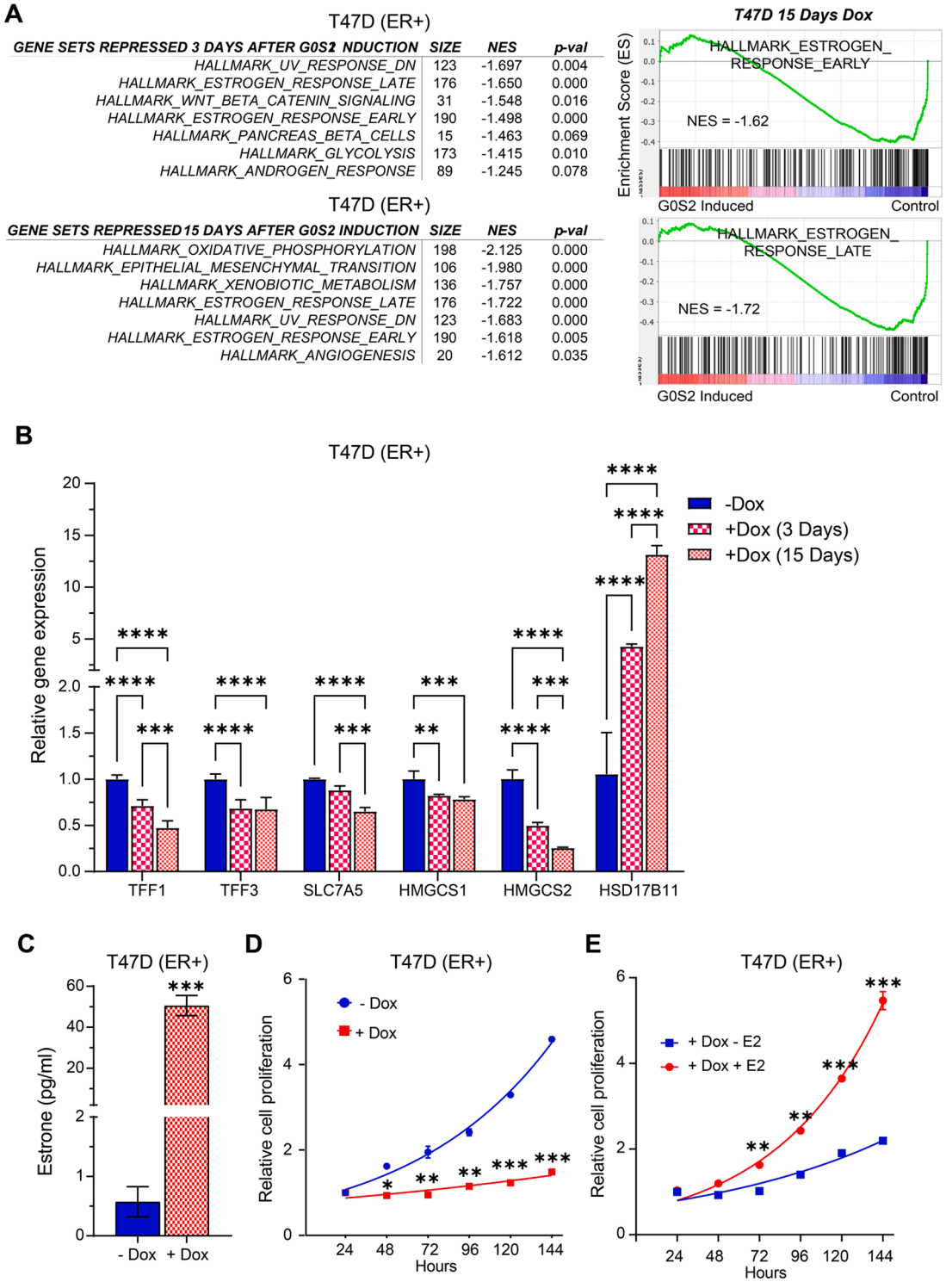

Fig. 3. G0S2 expression downregulates expression of ER target genes and alters expression of genes involved in estrogen regulation. (A) Gene set enrichment analysis (GSEA) showing the top 7 HALLMARK gene sets ranked by normalized enrichment score (NES) downregulated in T47D cells at 3 and 15 days of G0S2 induction. Representative gene set enrichment plots for ESTROGEN_RESPONSE_EARLY and ESTROGEN_RESPONSE_LATE. (B) Real-time PCR confirmation of repression of estrogen receptor target genes TFF1, TFF3 and SLC7A5 and steroid biosynthetic enzymes HMGCS1 and HMGCS2, and induction of estradiol converting enzyme HSD17B11 after G0S2 induction in T47D cells. Data represent mean +/- standard error of the mean of three biological replicates. Two-tailed student's t-tests were performed for statistical analysis. Experiments were repeated at least twice with similar results. (C) G0S2 induction in T47D cells resulted in increased levels of estrone. Media estrone levels were assessed after 5-day induction of G0S2. Cells were cultured in 1 pM estradiol containing media. (D) G0S2 induction in T47D cells resulted in a dramatic decrease in cell proliferation with estrogen depletion. T47D cells were induced for G0S2 expression for 15 days and then assessed for cell proliferation in estrogen depleted media. (E) Decreased cell proliferation with G0S2 induction and estrogen depletion in T47D cells could be rescued by addition of estradiol. T47D cells were induced for G0S2 expression for 15 days and then assessed for cell proliferation in estrogen depleted media or estrogen depleted media supplemented with 10 nM estradiol (E2). Data was normalized to the 24-hour time point. Two-tailed student's t-tests were performed for statistical analysis. $^{*}P \leq 0.05$, $^{**}P \leq 0.01$, $^{***}P \leq 0.005$, $^{****}P \leq 0.001$.

alteration in ER target genes and HSD17B11 expression when assessed by RT-PCR (Figure S2). As expected, while estrone levels were induced in MDA-MB-231 cells, this did not negatively impact MDA-MB-231 cell proliferation as these cells are not dependent on estrogen for growth (Figure S2). In summary, G0S2 induction led to an antiestrogen effect including repression of ER target gene expression that is in turn associated with altered estradiol biosynthesis and metabolism.

Expression of G0S2-altered estrogen biosynthesis and metabolic genes correlates with patient survival and G0S2 expression in patient samples

To assess the clinical relevance that G0S2 may have an antiestrogenic effect in breast cancer, we interrogated G0S2, HSD17B11, and HMGSC1 expression levels in the publicly available METABRIC database through cBioPortal [46]. Patients with G0S2 expression 1.0 standard deviations above the mean or greater had better relapse-free survival, consistent with our prior findings (Fig. 4A) [32,33]. Those patients with levels of the estradiol metabolizing enzyme HSD17B11 1.0 standard deviations above the mean also had a relapse survival advantage. In contrast, those patients with higher levels of the cholesterol biosynthetic pathway enzyme, HMGSC1, had lower relapse survival (Fig. 4A). Consistent with the situation in G0S2 induced T47D cells, there was a significant positive correlation between G0S2 and HSD17B11 expression and a negative correlation between G0S2 and HMGCS1 expression in breast cancer patient samples from the METABRIC cohort (Fig. 4B). These findings support the notion that G0S2 alters the expression of estrogen biosynthesis and metabolic genes that provides a net antiestrogenic effect and increased relapse free survival in breast cancer patients.

G0S2 promotes metastasis in ER- MMTV-PYMT mice

To assess the role of G0S2 in breast cancer in vivo we chose the well-characterized mouse mammary tumor virus (MMTV) driven polyoma middle T antigen (PyMT), MMTV-PyMT model. This model was chosen because while there are limited genetically engineered models of ER+ breast cancer, the MMTV model has been suggested to be at least partially dependent on estrogen during the early stages of tumorigenesis; however, the tumors in these mice ultimately become ER-negative and estrogen independent [41,47]. We crossed MMTV-PyMT mice with previously described G0S2 null mice [16]. The phenotype observed was consistent with the hypothesis that G0S2 functions as a tumor promoter in ER- breast cancer. There was a modest but significant increase in tumor latency but no change in tumor progression in mice with deleted G0S2 compared to G0S2 wild-type mice (Figs. 5A and 5B). Further, there was a non-significant decreased trend for largest and overall tumor weight in G0S2 null mice (Fig. 5C and 5D). The largest observed effect was on lung metastasis with G0S2 deleted mice having a substantially lower incidence of lung metastases compared to G0S2 wildtype mice (Fig. 5E). Together, the data supports the in vitro findings that G0S2 promotes cell proliferation and cell migration in ER- MDA.MB-231 cells.

Discussion

Previous studies have demonstrated both tumor-suppressive and oncogenic effects of G0S2. However, studies on G0S2 specific to breast cancer have been few. We recently reported a role for G0S2 in ER+ breast cancer suppression as low G0S2 expression correlated with increased recurrence after antiestrogen therapy and increased G0S2 expression sensitized ER+ breast cancer cells to tamoxifen and PI3K/mTOR inhibitors [33]. However, low G0S2 expression did not correlate with increased recurrence in ER- breast cancer patients, and a recent study reported that G0S2 knockdown in MDA-MB-231 cells repressed cell proliferation, cell migration, and EMT [38]. Hence, it appears that G0S2 may have cancer-type dependent effects including disparate effects in ER+ and ER- cancers. In this report, we dissected the role of G0S2 in ER+ versus ER- breast cancer and performed unbiased transcriptomic analysis to address mechanisms of G0S2 actions.

Overexpression of G0S2 in ER- breast cancer cells increased cell

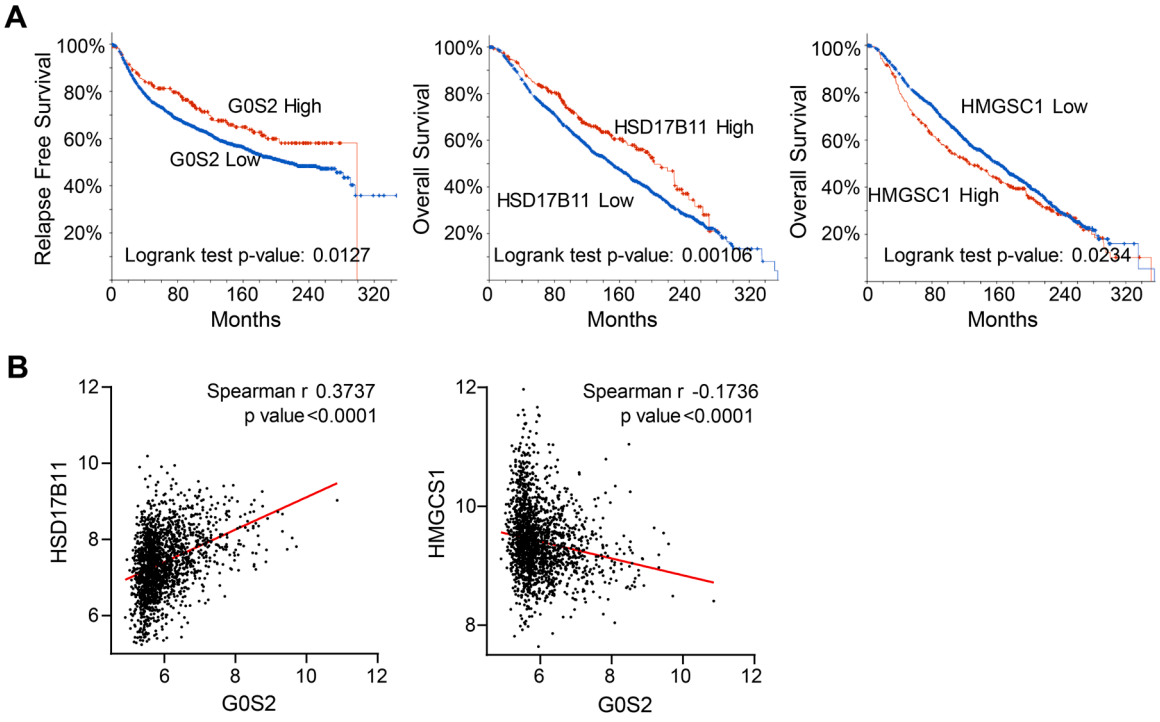

Fig. 4. Expression of G0S2-altered estrogen biosynthetic and metabolic genes correlates with patient survival and G0S2 expression in patient samples. (A) High expression of G0S2 and HSD17B11 is associated with improved survival of breast cancer patients, while high expression of HMGCS1 is associated with decreased survival. In each case high expression is defined as 1.0 SD above the mean. METABRIC data set (1903 patients) downloaded from cBioPortal. (B) G0S2 expression is positively correlated with HSD17B11 expression and inversely correlated with HMGCS1 expression in the METABRIC dataset.

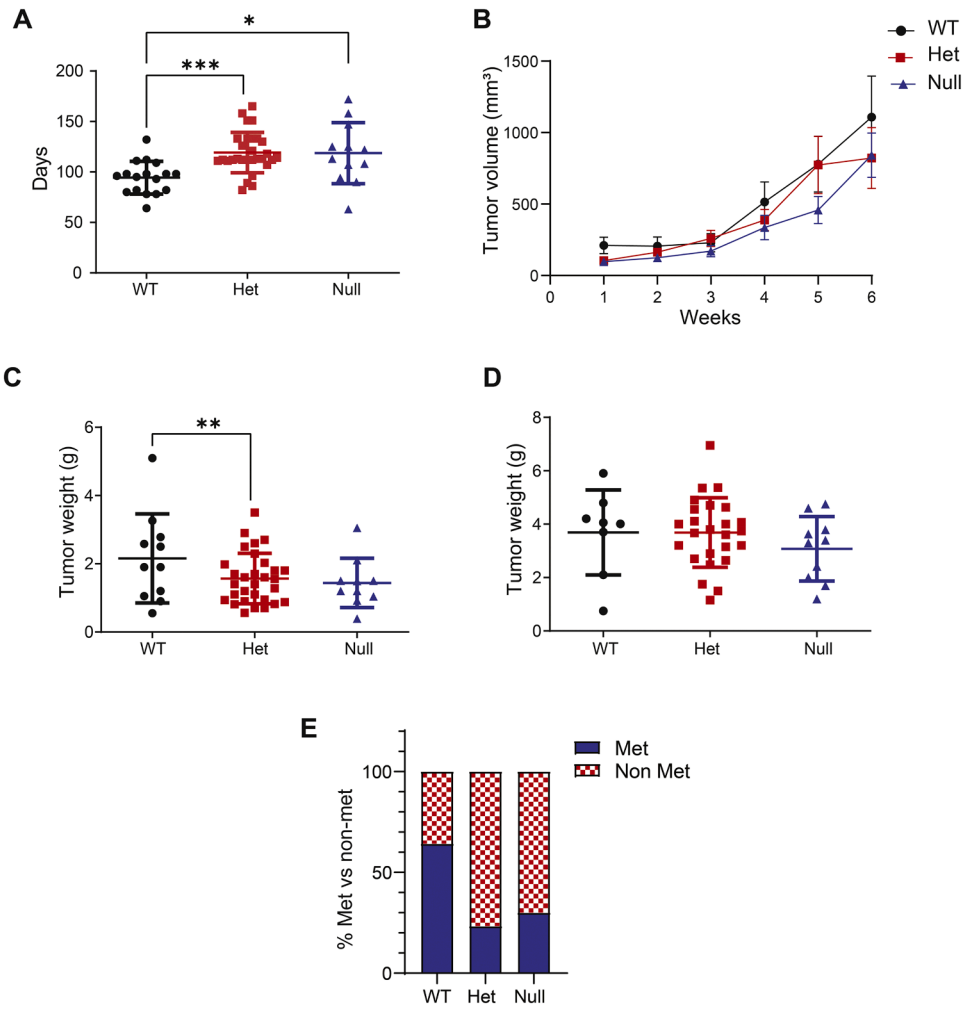

Fig. 5. G0S2 increased breast cancer metastasis of ER- MMTV-PyMT mouse tumors. MMTV-PyMT mice wildtype (WT), heterozygous (Het), and null (Mut) for G0S2 were assessed for primary tumor latency (A) and progression (B). G0S2 deletion resulted in increased tumor latency (first appearance of breast tumors) but no change in tumor progression (growth of primary tumors once established). G0S2 status also had minimal effects on total tumor weight (C) and largest tumor weight (D) at 6 weeks from first appearance. (E) G0S2 null mice had fewer lung metastasis. Percentage of mice with lung metastasis (Met) 6 weeks after first appearance of primary tumors, WT, $n = 14$; Het, $n = 30$; Mut, $n = 10$.

proliferation and cell migration, which was associated with repression of epithelial markers consistent with induction of EMT, including the repression of E-cadherin, whose lost function or expression has been implicated in cancer progression and metastasis [48]. These findings are highly consistent with the work of Cho et al. who reciprocally reported decreased cell proliferation and cell migration and induction of E-cadherin in G0S2 knockdown MDA-MB-231 cells [38]. This may also explain why G0S2 expression appears to corelate with a more aggressive phenotype in ER- breast cancer patients [32,38]. In stark contrast, we found that induction of G0S2 in ER+ cells resulted in decreased cell proliferation and repression of cell migration. This was associated with genome-wide repression of estrogen receptor targets genes indicating that G0S2 may inhibit estrogen signaling in breast cancer cells, which may explain our prior and current findings that G0S2 has antitumor activity in ER+ cells and is associated with decreased recurrence in ER+ breast cancer patients [32,33].

Interestingly, on a transcriptomics level, we found evidence for G0S2 promoting EMT and antagonizing ER signaling in both ER- and ER+ breast cancer cells. However, this appears to manifest as overall tumor promotion in ER- cells and overall tumor inhibition in ER+ cells. This perhaps is due to the high estrogen-dependent nature of ER+ cells that dominates their ability to proliferate and survive, superseding any G0S2 mediated pro-migratory and invasive effects. Since ER- cells do not depend on estrogen for growth this antitumor effect would be predicted to not be present in ER- cells. This duality of G0S2 actions is predicted to have important clinical ramifications as the net effect of G0S2 targeting may be different in ER+ versus ER- cells. This is exemplified in our MMTV-PyMT ER- mouse experiments, which most clearly demonstrated a pro-metastatic activity for G0S2. Although G0S2 overexpression in ER- cells promoted cell proliferation, an effect on primary tumor growth was not detected in MMTV-PYMT G0S2 null mice. We speculate that one reason for this discrepancy may be that lipid metabolic effects of G0S2 may not manifest well on normal chow diet. Further experiments are required, including use of other human ER- and ER+ cell lines and mouse models and alternating fat diet content, to confirm the precise role of G0S2 in breast cancer.

A major novel finding of our work is that G0S2 appears to repress estrogen signaling and ER target gene expression perhaps by directly inhibiting 3-hydroxy-3-methylglutaryl-CoA synthases (HMGCS1 and HMGCS2), which condense acetyl-CoA with acetoacetyl-CoA to form 3-hydroxy-3-methylglutaryl-CoA (HMG-CoA) [40]. This reaction comprises the second step in the mevalonate-dependent isoprenoid biosynthesis pathway [40]. HMG-CoA is an intermediate in both cholesterol synthesis and ketogenesis [40]. This suggests that along with its well-established role in inhibiting lipolysis by inhibiting the activity of adipose triglyceride lipase (ATGL), G0S2 may also be involved in fine-tuning the mevalonate-dependent isoprenoid biosynthesis pathway, thus regulating the diverse class of isoprenoid derivatives including cholesterol, bile acids, vitamin D, retinoids and all steroid hormones [49]. Previous reports have indicated that the cholesterol metabolite, 27-hydroxycholesterol promotes metastasis through its effects on myeloid immune cells [50,51]. Since 27-hydroxychoelsterol levels typically mirror those of cholesterol, decreased cholesterol production capacity in G0S2 null mice may explain the decrease observed in

metastasis (Fig. 5E). Therefore, this combined action of G0S2 on ATGL and HMGCS1 would be a potential mechanism to decrease the utilization of acetyl-CoA, cholesterol and its metabolites, and promoting its storage as fat. In the future it would be interesting to comprehensively assess lipidomic alterations mediated by induction of G0S2.

Interestingly, the enzyme hydroxysteroid 17-beta dehydrogenase 11 (HSD17B11) that is known to convert estradiol to estrone was highly induced by G0S2 expression [43–45]. Estrone is 10- to 50-fold less potent than estradiol. For example, one study found the relative binding affinities of estrone for human ERα and ERβ were 4.0% and 3.5% compared to estradiol [52]. We confirmed that G0S2 overexpressing cells contained 40-fold more estrone than controls and that under estrogen limiting conditions, cell proliferation of G0S2 expressing cells is dramatically decreased. The potential wider-ranging implications of these finding await further studies, but it should be noted that prior studies involving G0S2 null mice have not reported differences in circulating levels of steroid hormones [14,16]. We hypothesize that G0S2 may limit local isoprenoid product bioavailability, including tumor levels of estradiol, to support ER+ breast cancer. This hypothesis is supported by our analysis where high G0S2 and HSD17B11 levels were associated with increased survival, while high levels of HMGCS1 was associated with worse survival.

Based on our findings we expect G0S2 knockout mice may have decreased estradiol and increased estrone levels in the mammary gland and perhaps have other local hormonal disturbances. An important follow-up experiment would be generating and analyzing mammary gland specific G0S2 KO mice and crossing G0S2 KO mice with ER-activity reporter mice to study the spatial and temporal effects of G0S2 on hormone dynamics in the mammary gland. Interestingly, G0S2 mice have a known lactation defect which would be consistent with local reproductive hormone dysregulation in the mammary gland [16].

Conclusions

In summary, our findings suggest that G0S2 may have a complex, breast cancer subtype-specific effect on breast cancer. Using unbiased *de novo* approaches, we found that G0S2 antagonized estrogen signaling in breast cancer cells which is associated with a proposed wider role for G0S2 in metabolic regulation beyond the regulation of lipolysis. If confirmed, these findings may have far-reaching implications on the functional significance of G0S2 in a variety cancers and other metabolic diseases. A full assessment of the cell type-dependent metabolic effects of G0S2 is warranted.

Data accessibility

The RNA-seq datasets for the current study have been submitted to the NCBI Database of GEO Datasets under the accession number GSE227698.

Funding

This work was supported by the National Institutes of Health grants R01-CA211875 (MJS), R03CA223709 (MJS), R01CA234025 (ERN) and a DOD PRCRP Impact Award W81XWH2110903 (MJS).

CRediT authorship contribution statement

Andrea K. Corbet: Conceptualization, Methodology, Validation, Formal analysis, Investigation, Data curation, Writing – original draft, Visualization, Supervision. **Emmanuel Bikorimana:** Methodology, Validation, Formal analysis, Investigation. **Raya I. Boyd:** Methodology, Investigation. **Doha Shokry:** Methodology, Investigation. **Kelly Kries:** Methodology, Investigation. **Ayush Gupta:** Methodology, Investigation. **Anneliese Paton:** Methodology, Investigation. **Zhengyang Sun:** Validation. **Zeeshan Fazal:** Validation, Formal analysis, Data curation. **Sarah J. Freemantle:** Conceptualization, Writing – review & editing, Supervision, Project administration, Funding acquisition. **Erik R. Nelson:** Conceptualization, Writing – review & editing, Supervision. **Michael J. Spinella:** Conceptualization, Formal analysis, Writing – original draft, Writing – review & editing, Supervision, Project administration, Funding acquisition. **Ratnakar Singh:** Conceptualization, Methodology, Validation, Investigation, Data curation, Writing – review & editing, Visualization, Supervision, Project administration, Funding acquisition.

Declaration of Competing Interest

The authors declare that they have no known competing financial interests or personal relationships that could have appeared to influence the work reported in this paper.

Acknowledgments

We would like to thank members of the Roy J. Carver Biotechnology Center at the University of Illinois, including Dr. Alvaro Hernandez and Chris Wright for RNA sequencing. We would also like to thank the High-Performance Biological Computing (HPCBio) group at the University of Illinois, including Jenny Drnevich and Jessica Holmes for help with bioinformatics.

Supplementary materials

Supplementary material associated with this article can be found, in the online version, at doi:10.1016/j.tranon.2023.101676.

References

[1] A.N. Giaquinto, H. Sung, K.D. Miller, J.L. Kramer, L.A. Newman, A. Minihan, A. Jemal, R.L. Siegel, Breast cancer statistics, 2022, CA Cancer J. Clin. 72 (6) (2022) 524–541, https://doi.org/10.3322/caac.21754. Epub 2022 Oct 3PMID: 36190501.

[2] R. Beňačka, D. Szabóová, Z. Guľašová, Z. Hertelyová, J. Radoňák, Classic and new markers in diagnostics and classification of breast cancer, Cancers (Basel) 14 (21) (2022) 5444, https://doi.org/10.3390/cancers14215444. PMID: 36358862PMCID: PMC9654192.

[3] P.H. Lin, G. Laliotis, The present and future of clinical management in metastatic breast cancer, J. Clin. Med. 11 (19) (2022) 5891, https://doi.org/10.3390/jcm11195891. PMID: 36233758PMCID: PMC9573678.

[4] A. Ignatov, H. Eggemann, E. Burger, T. Ignatov, Patterns of breast cancer relapse in accordance to biological subtype, J. Cancer Res. Clin. Oncol. 144 (7) (2018) 1347–1355, https://doi.org/10.1007/s00432-018-2644-2. Epub 2018 Apr 19PMID: 29675790.

[5] D. Musheyev, A. Alayev, Endocrine therapy resistance: what we know and future directions, Explor. Target Antitumor. Ther. 3 (4) (2022) 480–496, https://doi.org/10.37349/etat.2022.00096. Epub 2022 Aug 31PMID: 360719.

[6] L. Russell, D.R. Forsdyke, A human putative lymphocyte G0/G1 switch gene containing a CpG-rich island encodes a small basic protein with the potential to be phosphorylated, DNA Cell Biol. 10 (8) (1991) 581–591, https://doi.org/10.1089/dna.1991.10.581. PMID: 1930693.

[7] B.L. Heckmann, X. Zhang, X. Xie, J. Liu, The G0/G1 switch gene 2 (G0S2): regulating metabolism and beyond, Biochim. Biophys. Acta 1831 (2) (2013) 276–281, https://doi.org/10.1016/j.bbalip.2012.09.016. Epub 2012 Sep 29. PMID: 23032787PMCID: PMC3698047.

[8] B.L. Heckmann, X. Zhang, A.M. Saarinen, J. Liu, Regulation of G0/G1 Switch Gene 2 (G0S2) protein ubiquitination and stability by triglyceride accumulation and ATGL interaction, PLoS One 11 (6) (2016), e0156742, https://doi.org/10.1371/journal.pone.0156742. PMID: 27248498PMCID: PMC4889065.

[9] M.W. Moran, E.P. Ramirez, J.D. Zook, A.M. Saarinen, B. Baravati, M.R. Goode, V. Laloudakis, E.K. Kaschner, T.L. Olson, F.M. Craciunescu, D.T. Hansen, J. Liu, P. Fromme, Biophysical characterization and a roadmap towards the NMR solution structure of G0S2, a key enzyme in non-alcoholic fatty liver disease, PLoS One 16 (7) (2021), e0249164, https://doi.org/10.1371/journal.pone.0249164. PMID: 34260600PMCID: PMC8279337.

[10] X. Zhang, B.L. Heckmann, L.E. Campbell, J. Liu, G0S2: a small giant controller of lipolysis and adipose-liver fatty acid flux, Biochim. Biophys. Acta Mol Cell Biol Lipids 1862 (10 Pt B) (2017) 1146–1154, https://doi.org/10.1016/j.bbalip.2017.06.007. Epub 2017 Jun 21PMID: 28645852PMCID: PMC5890940.

[11] N. Matsunaga, E. Ikeda, K. Kakimoto, M. Watanabe, N. Shindo, A. Tsuruta, H. Ikeyama, K. Hamamura, K. Higashi, T. Yamashita, H. Kondo, Y. Yoshida, M. Matsuda, T. Ogino, K. Tokushige, K. Itcho, Y. Furuichi, T. Nakao, K. Yasuda, A. Doi, T. Amamoto, H. Aramaki, M. Tsuda, K. Inoue, A. Ojida, S. Koyanagi,

S. Ohdo, Inhibition of G0/G1 switch 2 ameliorates renal inflammation in chronic kidney disease, EBioMedicine 13 (2016) 262–273, https://doi.org/10.1016/j.ebiom.2016.10.008. Epub 2016 Oct 6PMID: 27745900PMCID: PMC5264248.

[12] L. Xu, Z. Li, Y. Li, Z. Luo, Y. Luo, B. Xiao, H. Yang, The expression pattern and regulatory mechanism of the G0/G1 Switch Gene 2 (*G0S2*) in the pathogenesis and treatment of AChR myasthenia gravis (MG), Mediators Inflamm. 2020 (2020), 4286047, https://doi.org/10.1155/2020/4286047. PMID: 33061827PMCID: PMC7545457.

[13] R. Zhang, J. Meng, S. Yang, W. Liu, L. Shi, J. Zeng, J. Chang, B. Liang, N. Liu, D. Xing, Recent advances on the role of ATGL in cancer, Front. Oncol. 12 (2022), 944025, https://doi.org/10.3389/fonc.2022.944025. PMID: 35912266PMCID: PMC9326118.

[14] X. Yang, X. Lu, M. Lombès, G.B. Rha, Y.I. Chi, T.M. Guerin, E.J. Smart, J. Liu, The G(0)/G(1) switch gene 2 regulates adipose lipolysis through association with adipose triglyceride lipase, Cell Metab. 11 (3) (2010) 194–205, https://doi.org/10.1016/j.cmet.2010.02.003. PMID: 20197052PMCID: PMC3658843.

[15] M. Schweiger, M. Paar, C. Eder, J. Brandis, E. Moser, G. Gorkiewicz, S. Grond, F. P. Radner, I. Cerk, I. Cornaciu, M. Oberer, S. Kersten, R. Zechner, R. Zimmermann, A. Lass, G0/G1 switch gene-2 regulates human adipocyte lipolysis by affecting activity and localization of adipose triglyceride lipase, J. Lipid Res. 53 (11) (2012) 2307–2317, https://doi.org/10.1194/jlr.M027409. Epub 2012 Aug 13PMID: 22891293PMCID: PMC3466000.

[16] T. Ma, A.G. Lopez-Aguiar, A. Li, Y. Lu, D. Sekula, E.E. Nattie, S. Freemantle, E. Dmitrovsky, Mice lacking G0S2 are lean and cold-tolerant, Cancer Biol. Ther. 15 (5) (2014) 643–650, https://doi.org/10.4161/cbt.28251. Epub 2014 Feb 20PMID: 24556704PMCID: PMC4026087.

[17] X. Hu, H. Luo, C. Dou, X. Chen, Y. Huang, L. Wang, S. Xue, Z. Sun, S. Chen, Q. Xu, T. Geng, X. Zhao, H. Cui, Metformin triggers apoptosis and induction of the G0/G1 Switch 2 gene in macrophages, Genes (Basel) 12 (9) (2021) 1437, https://doi.org/10.3390/genes12091437. PMID: 34573418PMCID: PMC8468785.

[18] D.R. Mohan, A.M. Lerario, T. Else, B. Mukherjee, M.Q. Almeida, M. Vinco, J. Rege, B.M.P. Mariani, M.C.N. Zerbini, B.B. Mendonca, A.C. Latronico, S.K.N. Marie, W. E. Rainey, T.J. Giordano, M.C.B.V. Fragoso, G.D. Hammer, Targeted assessment of *G0S2* methylation identifies a rapidly recurrent, routinely fatal molecular subtype of adrenocortical carcinoma, Clin. Cancer Res. 25 (11) (2019) 3276–3288, https://doi.org/10.1158/1078-0432.CCR-18-2693. Epub 2019 Feb 15PMID: 30770352PMCID: PMC7117545.

[19] Y. Nobeyama, Y. Watanabe, H. Nakagawa, Silencing of G0/G1 switch gene 2 in cutaneous squamous cell carcinoma, PLoS One 12 (10) (2017), e0187047, https://doi.org/10.1371/journal.pone.0187047. PMID: 29073263PMCID: PMC5658152.

[20] J.W. Wu, C. Preuss, S.P. Wang, H. Yang, B. Ji, G.W. Carter, R. Gladdy, G. Andelfinger, G.A Mitchell, Epistatic interaction between the lipase-encoding genes Pnpla2 and Lipe causes liposarcoma in mice, PLos Genet. 13 (5) (2017), e1006716, https://doi.org/10.1371/journal.pgen.1006716. PMID: 28459858PMCID: PMC5432192.

[21] R. Zagani, W. El-Assaad, I. Gamache, J.G. Teodoro, Inhibition of adipose triglyceride lipase (ATGL) by the putative tumor suppressor G0S2 or a small molecule inhibitor attenuates the growth of cancer cells, Oncotarget 6 (29) (2015) 28282–28295, https://doi.org/10.18632/oncotarget.5061. PMID: 26318046PMCID: PMC4695060.

[22] J. Lippert, B. Altieri, B. Morrison, S. Steinhauer, G. Smith, A. Lorey, H. Urlaub, S. Kircher, A. Sitch, M. Fassnacht, C.L. Ronchi, Prognostic role of targeted methylation analysis in paraffin-embedded samples of adrenocortical carcinoma, J. Clin. Endocrinol. Metab. 107 (10) (2022) 2892–2899, https://doi.org/10.1210/clinem/dgac470. PMID: 35929659PMCID: PMC9516165.

[23] G. Sultan, S. Zubair, I.A. Tayubi, H.U. Dahms, I.H. Madar, Towards the early detection of ductal carcinoma (a common type of breast cancer) using biomarkers linked to the PPAR(γ) signaling pathway, Bioinformation 15 (11) (2019) 799–805, https://doi.org/10.6026/97320630015799. PMID: 31902979PMCID: PMC6936658.

[24] M. Kusakabe, K. Watanabe, N. Emoto, N. Aki, H. Kage, T. Nagase, J. Nakajima, Y. Yatomi, N. Ohishi, D. Takai, Impact of DNA demethylation of the G0S2 gene on the transcription of G0S2 in squamous lung cancer cell lines with or without nuclear receptor agonists, Biochem. Biophys. Res. Commun. 390 (4) (2009) 1283–1287, https://doi.org/10.1016/j.bbrc.2009.10.137. Epub 2009 Oct 28PMID: 19878646.

[25] M. Kusakabe, T. Kutomi, K. Watanabe, N. Emoto, N. Aki, H. Kage, E. Hamano, H. Kitagawa, T. Nagase, A. Sano, Y. Yoshida, T. Fukami, T. Murakawa, J. Nakajima, S. Takamoto, S. Ota, M. Fukayama, Y. Yatomi, N. Ohishi, D. Takai, Identification of G0S2 as a gene frequently methylated in squamous lung cancer by combination of in silico and experimental approaches, Int. J. Cancer 126 (8) (2010) 1895–1902, https://doi.org/10.1002/ijc.24947. PMID: 19816938.

[26] O. Barreau, G. Assié, H. Wilmot-Roussel, B. Ragazzon, C. Baudry, K. Perlemoine, F. René-Corail, X. Bertagna, B. Dousset, N. Hamzaoui, F. Tissier, A. de Reynies, J. Bertherat, Identification of a CpG island methylator phenotype in adrenocortical carcinomas, J. Clin. Endocrinol. Metab. 98 (1) (2013) E174–E184, https://doi.org/10.1210/jc.2012-2993. Epub 2012 Oct 23PMID: 23093492.

[27] H. Choi, H. Lee, T.H. Kim, H.J. Kim, Y.J. Lee, S.J. Lee, J.H. Yu, D. Kim, K.S. Kim, S. W. Park, J.W. Kim, G0/G1 switch gene 2 has a critical role in adipocyte differentiation, Cell Death Differ. 21 (7) (2014) 1071–1080, https://doi.org/10.1038/cdd.2014.26. Epub 2014 Feb 28PMID: 24583640PMCID: PMC4207475.

[28] T. Yamada, C.S. Park, Y. Shen, K.R. Rabin, H.D. Lacorazza, G0S2 inhibits the proliferation of K562 cells by interacting with nucleolin in the cytosol, Leuk. Res. 38 (2) (2014) 210–217, https://doi.org/10.1016/j.leukres.2013.10.006. Epub 2013 Oct 14PMID: 24183236PMCID: PMC3946941.

[29] C. Welch, M.K. Santra, W. El-Assaad, X. Zhu, W.E. Huber, R.A. Keys, J.G. Teodoro, M.R. Green, Identification of a protein, G0S2, that lacks Bcl-2 homology domains and interacts with and antagonizes Bcl-2, Cancer Res. 69 (17) (2009) 6782–6789, https://doi.org/10.1158/0008-5472.CAN-09-0128. Epub 2009 Aug 25PMID: 19706769PMCID: PMC2841785.

[30] S. Kitareewan, S. Blumen, D. Sekula, R.P. Bissonnette, W.W. Lamph, Q. Cui, R. Gallagher, E. Dmitrovsky, G0S2 is an all-trans-retinoic acid target gene, Int. J. Oncol. 33 (2) (2008) 397–404. PMID: 18636162PMCID: PMC2597086.

[31] F. Zhang, Y.L. Zhu, W.L. Deng, J. Zhu, J. Zhang, Activation of *G0S2* is coordinated by recruitment of PML/RARα and C/EBPε to its promoter during ATRA-induced APL differentiation, J. Leukoc Biol. 101 (3) (2017) 655–664, https://doi.org/10.1189/jlb.1A0316-116R. Epub 2016 Sep 7PMID: 27605212.

[32] C.Y. Yim, D.J. Sekula, M.P. Hever-Jardine, X. Liu, J.M. Warzecha, J. Tam, S. J. Freemantle, E. Dmitrovsky, M.J. Spinella, G0S2 Suppresses oncogenic transformation by repressing a MYC-regulated transcriptional program, Cancer Res. 76 (5) (2016) 1204–1213, https://doi.org/10.1158/0008-5472.CAN-15-2265. Epub 2016 Feb 2PMID: 26837760PMCID: PMC4775337.

[33] C.Y. Yim, E. Bikorimana, E. Khan, J.M. Warzecha, L. Shin, J. Rodriguez, E. Dmitrovsky, S.J. Freemantle, M.J. Spinella, G0S2 represses PI3K/mTOR signaling and increases sensitivity to PI3K/mTOR pathway inhibitors in breast cancer, Cell Cycle 16 (21) (2017) 2146–2155, https://doi.org/10.1080/15384101.2017.1371884. Epub 2017 Sep 14PMID: 28910567PMCID: PMC5731418.

[34] R. Zagani, I. Gamache, J.G. Teodoro, Deletion of the putative tumor suppressor gene, G0s2, does not affect progression of Eμ-Myc driven lymphomas in mice, Leuk. Res. 40 (2016) 100–102, https://doi.org/10.1016/j.leukres.2015.11.011. Epub 2015 Dec 2PMID: 26654706.

[35] Y. Wang, Y. Hou, W. Zhang, A.A. Alvarez, Y. Bai, B. Hu, S.Y. Cheng, K. Yang, Y. Li, H Feng, Lipolytic inhibitor G0S2 modulates glioma stem-like cell radiation response, J. Exp. Clin. Cancer Res. 38 (1) (2019) 147, https://doi.org/10.1186/s13046-019-1151-x. Erratum in: J Orthop Surg Res. 2019 Jul 16;14(1):215. Erratum in: J Exp Clin Cancer Res. 2019 Jul 29;38(1):331. PMID: 30953555; PMCID: PMC6451284.

[36] T. Fukunaga, Y. Fujita, H. Kishima, T. Yamashita, Methylation dependent down-regulation of G0S2 leads to suppression of invasion and improved prognosis of IDH1-mutant glioma, PLoS One 13 (11) (2018), e0206552, https://doi.org/10.1371/journal.pone.0206552. PMID: 30388142PMCID: PMC6214530.

[37] D. Cheishvili, B. Stefanska, C. Yi, C.C. Li, P. Yu, A. Arakelian, I. Tanvir, H.A. Khan, S. Rabbani, M. Szyf, A common promoter hypomethylation signature in invasive breast, liver and prostate cancer cell lines reveals novel targets involved in cancer invasiveness, Oncotarget 6 (32) (2015) 33253–33268, https://doi.org/10.18632/oncotarget.5291. PMID: 26427334PMCID: PMC4741763.

[38] E. Cho, Y.J. Kwon, D.J. Ye, H.S. Baek, T.U. Kwon, H.K. Choi, Y.J. Chun, G0/G1 Switch 2 induces cell survival and metastasis through integrin-mediated signal transduction in human invasive breast cancer cells, Biomol. Ther. 27 (6) (2019) 591–602, https://doi.org/10.4062/biomolther.2019.063. Epub ahead of printPMID: 31272137PMCID: PMC6824625.

[39] R. Singh, Z. Fazal, E. Bikorimana, R.I. Boyd, C. Yerby, M. Tomlin, H. Baldwin, D. Shokry, A.K. Corbet, K. Shahid, A. Hattab, S.J. Freemantle, M.J. Spinella, Reciprocal epigenetic remodeling controls testicular cancer hypersensitivity to hypomethylating agents and chemotherapy, Mol. Oncol. 16 (3) (2022) 683–698, https://doi.org/10.1002/1878-0261.13096. Epub 2021 Sep 15PMID: 34482638PMCID: PMC8807365.

[40] J.L. Goldstein, M.S. Brown, Regulation of the mevalonate pathway, Nature 343 (6257) (1990) 425–430, https://doi.org/10.1038/343425a0. PMID: 1967820.

[41] E.R. Nelson, S.E. Wardell, J.S. Jasper, S. Park, S. Suchindran, M.K. Howe, N. J. Carver, R.V. Pillai, P.M. Sullivan, V. Sondhi, M. Umetani, J. Geradts, D. P. McDonnell, 27-Hydroxycholesterol links hypercholesterolemia and breast cancer pathophysiology, Science 342 (6162) (2013) 1094–1098, https://doi.org/10.1126/science.1241908. PMID: 24288332PMCID: PMC3899689.

[42] C.D. DuSell, D.P. McDonnell, 27-Hydroxycholesterol: a potential endogenous regulator of estrogen receptor signaling, Trends Pharmacol. Sci. 29 (10) (2008) 510–514, https://doi.org/10.1016/j.tips.2008.07.003. Epub 2008 Aug 22PMID: 18722677PMCID: PMC2702440.

[43] T. Lundová, H. Štambergová, L. Zemanová, M. Svobodová, J. Havránková, M. Šafr, V. Wsól, Human dehydrogenase/reductase (SDR family) member 8 (DHRS8): a description and evaluation of its biochemical properties, Mol. Cell. Biochem. 411 (1–2) (2016) 35–42, https://doi.org/10.1007/s11010-015-2566-0. Epub 2015 Oct 16PMID: 26472732.

[44] Z. Chai, P. Brereton, T. Suzuki, H. Sasano, V. Obeyesekere, G. Escher, R. Saffery, P. Fuller, C. Enriquez, Z. Krozowski, 17 beta-hydroxysteroid dehydrogenase type XI localizes to human steroidogenic cells, Endocrinology (2003).

[45] P. Brereton, T. Suzuki, H. Sasano, K. Li, C. Duarte, V. Obeyesekere, F. Haeseleer, K. Palczewski, I. Smith, P. Komesaroff, Z. Krozowski, Pan1b (17betaHSD11)-enzymatic activity and distribution in the lung, Mol. Cell. Endocrinol. 171 (1–2) (2001) 111–117, https://doi.org/10.1016/s0303-7207(00)00417-2. PMID: 11165019.

[46] B. Pereira, S.F. Chin, O.M. Rueda, H.K. Vollan, E. Provenzano, H.A. Bardwell, M. Pugh, L. Jones, R. Russell, S.J. Sammut, D.W. Tsui, B. Liu, S.J. Dawson, J. Abraham, H. Northen, J.F. Peden, A. Mukherjee, G. Turashvili, A.R. Green, S. McKinney, A. Oloumi, S. Shah, N. Rosenfeld, L. Murphy, D.R. Bentley, I.O. Ellis, A. Purushotham, S.E. Pinder, A.L. Børresen-Dale, H.M. Earl, P.D. Pharoah, M. T. Ross, S. Aparicio, C. Caldas, The somatic mutation profiles of 2,433 breast cancers refines their genomic and transcriptomic landscapes, Nat. Commun. 7 (2016) 11479, https://doi.org/10.1038/ncomms11479. PMID: 27161491PMCID: PMC4866047.

[47] T.H. Qiu, G.V. Chandramouli, K.W. Hunter, N.W. Alkharouf, J.E. Green, E.T. Liu, Global expression profiling identifies signatures of tumor virulence in MMTV-PyMT-transgenic mice: correlation to human disease, Cancer Res. 64 (17) (2004) 5973–5981, https://doi.org/10.1158/0008-5472.CAN-04-0242. PMID: 15342376.

[48] S.N. Rubtsova, I.Y. Zhitnyak, N.A. Gloushankova, Dual role of E-cadherin in cancer cells, Tissue Barriers 10 (4) (2022), 2005420, https://doi.org/10.1080/21688370.2021.2005420. Epub 2021 Nov 25PMID: 34821540PMCID: PMC9621038.

[49] A.H. Payne, D.B. Hales, Overview of steroidogenic enzymes in the pathway from cholesterol to active steroid hormones, Endocr. Rev. 25 (6) (2004) 947–970, https://doi.org/10.1210/er.2003-0030. PMID: 15583024.

[50] A.E. Baek, Y.A. Yu, S. He, S.E. Wardell, C.Y. Chang, S. Kwon, R.V. Pillai, H. B. McDowell, J.W. Thompson, L.G. Dubois, P.M. Sullivan, J.K. Kemper, M.D. Gunn, D.P. McDonnell, E.R. Nelson, The cholesterol metabolite 27 hydroxycholesterol facilitates breast cancer metastasis through its actions on immune cells, Nat. Commun. 8 (1) (2017) 864, https://doi.org/10.1038/s41467-017-00910-z. PMID: 29021522PMCID: PMC5636879.

[51] L. Ma, L. Wang, A.T. Nelson, C. Han, S. He, M.A. Henn, K. Menon, J.J. Chen, A. E. Baek, A. Vardanyan, S.H. Shahoei, S. Park, D.J. Shapiro, S.G. Nanjappa, E. R. Nelson, 27-Hydroxycholesterol acts on myeloid immune cells to induce T cell dysfunction, promoting breast cancer progression, Cancer Lett. 493 (2020) 266–283, https://doi.org/10.1016/j.canlet.2020.08.020. Epub 2020 Aug 28PMID: 32861706PMCID: PMC7572761.

[52] A. Escande, A. Pillon, N. Servant, J.P. Cravedi, F. Larrea, P. Muhn, J.C. Nicolas, V. Cavaillès, P. Balaguer, Evaluation of ligand selectivity using reporter cell lines stably expressing estrogen receptor alpha or beta, Biochem. Pharmacol. 71 (10) (2006) 1459–1469, https://doi.org/10.1016/j.bcp.2006.02.002. Epub 2006 Mar 22PMID: 16554039.